

# Review of the Silicon Oxide and Polysilicon Layer as the Passivated Contacts for TOPCon Solar Cells

Mengmeng Chu<sup>1</sup>, Muhammad Quddamah Khokhar<sup>2</sup>, Hasnain Yousuf<sup>1</sup>,  
Xinyi Fan<sup>1</sup>, Seungyong Han<sup>2</sup>, Youngkuk Kim<sup>3</sup>, Suresh Kumar Dhungel<sup>3</sup> ,  
and Junsin Yi<sup>3</sup> 

<sup>1</sup> Interdisciplinary Program in Photovoltaic System Engineering, Sungkyunkwan University, Suwon 16419, Korea

<sup>2</sup> Department of Electrical and Computer Engineering, Sungkyunkwan University, Suwon 16419, Korea

<sup>3</sup> College of Information and Communication Engineering, Sungkyunkwan University, Suwon 16419, Korea

(Received March 14, 2023; Accepted March 30, 2023)

**Abstract:** p-type Tunnel Oxide Passivating Contacts (TOPCon) solar cell is fabricated with a poly-Si/SiO<sub>x</sub> structure. It simultaneously achieves surface passivation and enhances the carriers' selective collection, which is a promising technology for conventional solar cells. The quality of passivation is depended on the quality of the tunnel oxide layer at the interface with the c-Si wafer, which is affected by the bond of SiO formed during the subsequent annealing process. The highest cell efficiency reported to date for the laboratory scale has increased to 26.1%, fabricated by the Institute for Solar Energy Research. The cells used a p-type float zone silicon with an interdigitated back contact (IBC) structure that fabricates poly-Si and SiO<sub>x</sub> layer achieves the highest implied open-circuit voltage ( $iV_{oc}$ ) is 750 mV, and the highest level of edge passivation is 40%. This review presents an overview of p-type TOPCon technologies, including the ultra-thin silicon oxide layer (SiO<sub>x</sub>) and poly-silicon layer (poly-Si), as well as the advancement of the SiO<sub>x</sub> and poly-Si layers. Subsequently, the limitations of improving efficiency are discussed in detail. Consequently, it is expected to provide a basis for the simplification of industrial mass production.

**Keywords:** p-type TOPCon, Silicon oxide, Polysilicon, Efficiency improving

## 1. INTRODUCTION

Solar energy is one of the most important renewable energies that converts into sustainable electricity by using solar cells to meet the ever-growing demand for sustainable energy in the world [1,2]. However, in various photovoltaic devices used for solar cells, crystalline silicon (c-Si) cells

account for ~90% market segment. Solar cells consist of semiconductor materials, carrier-selective contact (CSC) layers, that absorb photons from the electromagnetic spectrum and generate charge carriers of opposite polarity, electrons (n), and holes (p), whose flow produces photocurrent [3-5]. The mechanism of photovoltaic cells is shown in Fig. 1. Carrier separation is due to an electrochemical gradient formed by selective contact of holes and electrons adjacent to the absorber [6]. Failure to collect charge carriers results in electron-hole recombination, which reduces the effective carrier lifetime.

The efficiency of solar cells increases by an average of 0.5~0.6% per year and has exceeded 26% at present, but when

---

✉ Junsin Yi; [junsin@skku.edu](mailto:junsin@skku.edu)

Suresh Kumar Dhungel; [suresh@skku.edu](mailto:suresh@skku.edu)

Copyright ©2023 KIEEME. All rights reserved.

This is an Open-Access article distributed under the terms of the Creative Commons Attribution Non-Commercial License (<http://creativecommons.org/licenses/by-nc/3.0>) which permits unrestricted non-commercial use, distribution, and reproduction in any medium, provided the original work is properly cited.

the photoelectric conversion efficiency is close to 23%, the dominant efficiency loss is due to metal contacts [7]. Recombination losses [8,9] at the crystalline silicon (c-Si) surface and the interface of metal/Si contact are mainly caused by structural defects (crystal interfaces, impurities) or surface defects (dangling bonds at the c-Si surface) of the c-Si and parasitic absorption losses in the metallic reflector of rear-passivated silicon solar cells [10], which is the most important detrimental factor affecting the photovoltaics efficiency of solar cells.

Tunnel Oxidation Passivating Contact (TOPCon) solar cells feature a nano silicon oxide ( $\text{SiO}_x$ ) layer and phosphorus heavily doped poly-silicon ( $n^+$ -poly-Si) or boron-doped poly-silicon ( $p^+$ -poly-Si) layer simultaneously achieves excellent surface passivation and carrier selective collection [11]. The photovoltaic efficiency of TOPCon passivated solar cells has increased about 0.5~0.6% annually from the structure invented by Fraunhofer in 2013. Martin A Green *et al.* [12] reported the highest efficiency of the p-type PERC crystalline solar cell is  $26.0 \pm 0.5\%$  produced by FhG-ISE (test date 11/19). Sourav Sathukhan *et al.* [13] illustrated the efficiency of p-type silicon solar cells with a fabricated bifacial tunnel oxide layer improved to 25.4%. TOPCon solar cells with a specific surface area of  $4 \text{ cm}^2$  produced by Fraunhofer ISE [14] with an efficiency of 25.8% were reported in 2018. The p-type POLO-IBC solar cell with a record high efficiency of about  $26.1 \pm 0.3\%$  (2/18) [15]. Junsin Yi *et al.* [7] reported the efficiency increase of solar cells and compared the efficiency of laboratory and industrial scales in recent years the results are shown in Fig. 2. and Table 1 illustrated the development of TOPCon solar cells. Consequently, TOPCon c-Si technologies are one of the most promising surface passivation technologies for the next generation of solar cells [13,16-18].

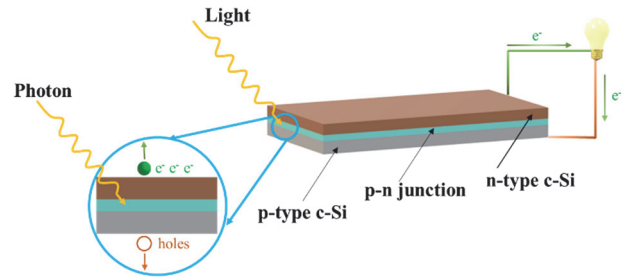


**Fig. 1.** The schematic diagram of the mechanism of the photovoltaic cells.

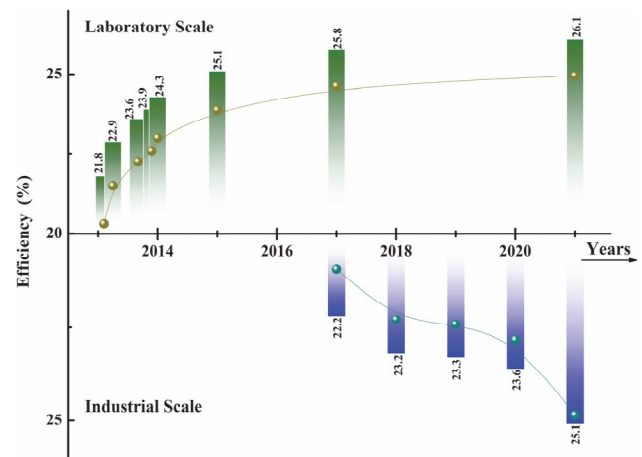


**Fig. 2.** Progress on TOPCon solar cell efficiencies on laboratory and industrial scale.

This work reviews the well-proven structure and methodology used to fabricate the passivation contact on p-type TOPCon solar cells. For this purpose, we discuss the  $\text{SiO}_x$  briefly between the wafer and poly-Si, elucidate the electrical architecture and various conceptual methods to prepare a high-quality poly-Si layer used to contact passivation, and provide recent promotion of surface passivation.

**Table 1.** The development of efficiency and  $V_{oc}$  for the TOPCon solar cells [19].

| Manufacture | Classification | Efficiency (%) | Voc (mV) | Area ( $\text{cm}^2$ ) | Certified by | Year |
|-------------|----------------|----------------|----------|------------------------|--------------|------|
| FhG-ISE     | p-TOPCon       | 26.00          | 732.3    | 4.015                  | FhG-ISE      | 2019 |
| FhG-ISE     | n-TOPCon       | 25.80          | 724.1    | 4.008                  | FhG-ISE      | 2017 |
| FhG-ISE     | n-TOPCon       | 22.95          | 700.0    | 244.4                  | FhG-ISE      | 2020 |
| ISFH        | p-POLO-IBC     | 26.10          | 726.6    | 3.986                  | ISFH         | 2018 |
| Trina       | n-TOPCon       | 24.58          | 716.8    | 244.6                  | ISFH         | 2020 |
| Jinko       | n-TOPCon       | 24.87          | 714.9    | 267.8                  | NREL         | 2020 |

## 2. TOPCon STRUCTURE

TOPCon consists of polysilicon (poly-Si)/silicon oxide ( $\text{SiO}_x$ ) stacks the structure is demonstrated in Fig. 3. Saw damage removal process (SDR) using potassium hydroxide (KOH) solution textured irregular pyramids on both sides.

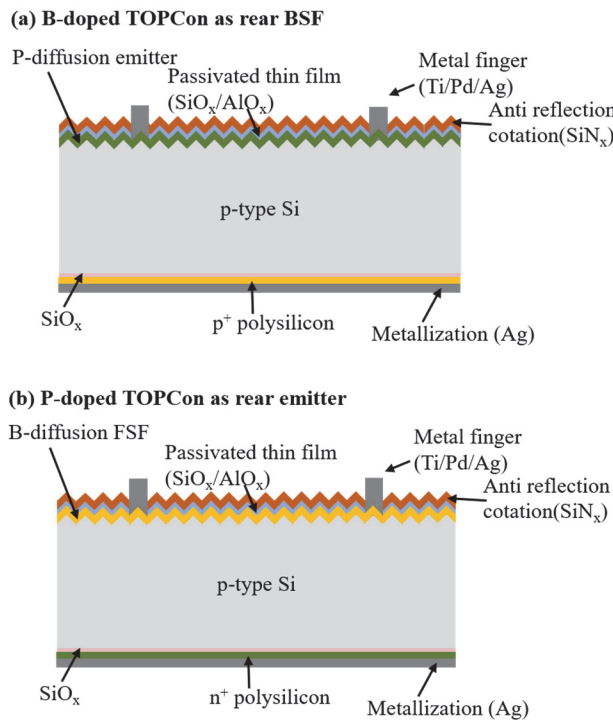


**Fig. 3.** Schematics of (a) front emitter and (b) rear emitter TOPCon solar cells with p-type c-Si wafers.

After the texturing process, the standard RCA cleaning is carried out to remove the oxides, organic contaminants, and metal ions on the wafer surface. The  $\text{p}^+$  boron emitter diffusion manipulates in a boron diffusion furnace with tribromide ( $\text{BBr}_3$ ) solution. To introduce the  $\text{SiO}_x$  layer, the single-side boron diffusion is removed by the etching process using hydrofluoric acid and nitric acid ( $\text{HF}/\text{HNO}_3$ ) solution. After that, the  $\text{SiO}_x$  tunneling layer and the polysilicon layer are developed gradually in the LPCVD system, and then the etching process eliminates the front side polysilicon. Subsequently, the additional RCA cleaning removes the chemicals on the surface, and the anti-reflection layer is coated. Finally, the screen-printed technology is designed for the metallization process [7]. The construction consists of a boron dopant emitter on the front side and a  $\text{SiO}_x$  tunnel passivating layer on the backside. Metal fingers fabricated on both sides, which were pasted by screen printing technology. The fabrication sequence is demonstrated in Fig. 4.

TOPCon technologies depend on the ultra-thin silicon oxide ( $\text{SiO}_x$ ) directly contacting the wafer, which reduces the dangling bonds density on the c-Si surface [20] and beneath the poly-Si layer attains excellent chemical passivation [9,21]. The chemical passivation of the  $\text{SiO}_x$  and the field passivation of the poly-Si can significantly reduce the recombination losses. The most dominant character of TOPCon structure is the tunnel passivated layer on the wafer surface, the thickness of  $\text{SiO}_x$  film is developed less than 2 nm, which ultrathin oxide layer can enhance the carriers transmitting [22]. At present, the simplest preparation method is to develop the oxide layer in a

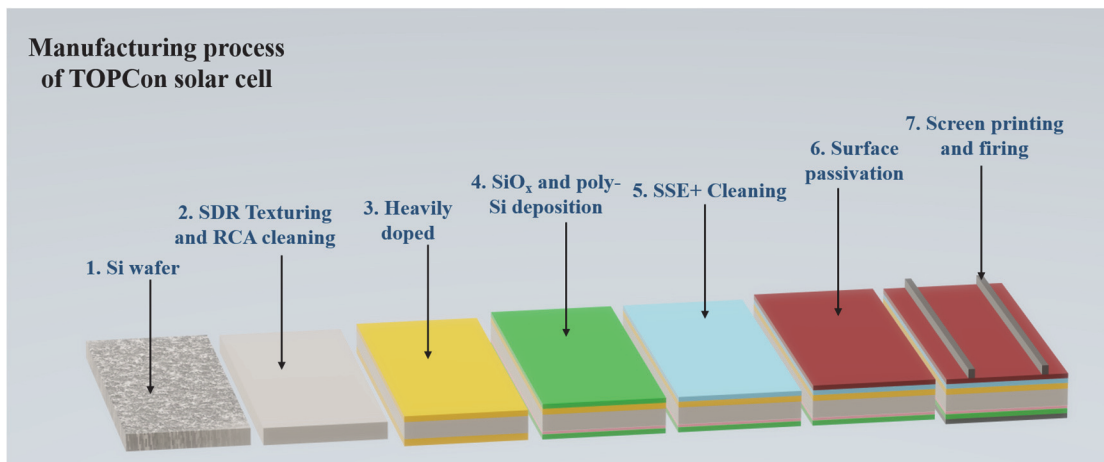


**Fig. 4.** Schematic of the production process of TOPCon solar cells [7].

wet and chemical acid mixture environment at over 90 °C [7]. Lots of hydrogen atoms in the highly doped poly-Si strengthen the passivation and significantly improve the conductivity of the majority of carriers. Therefore, the open circuit voltage ( $V_{oc}$ ) and fill factor (FF) of TOPCon cells are high.

### 3. Ultra-THIN SILICON OXIDE LAYER OF TOPCon

The thickness of the  $\text{SiO}_x$  layer is less than 2 nm to allow the tunneling transport of photocarriers [23,24]. Wang et al. [25], reported three thicknesses of the  $\text{SiO}_x$  layer as 1.25, 1.42 and, 1.55 nm, and found that when the  $\text{SiO}_x$  layer thickness is 1.55 nm, which attains excellent passivating behaviors with minimum saturation current ( $J_0$  about 18  $\text{fA}/\text{cm}^2$ ), and maximum value of fill factor and open circuit voltage (FF is 81.09%;  $V_{oc}$  is 687 mV). Tetravalent silicon ( $\text{Si}^{4+}$ ) is the most

important factor for the quality of the  $\text{SiO}_x$ , the higher proportion of  $\text{Si}^{4+}$  the better quality of the  $\text{SiO}_x$  passivation layer for p-type TOPCon [26]. The ultra-thin silicon oxide layers ( $\text{SiO}_x$ ) are grown by different techniques, as is shown in Fig. 5 a well-known and eco-friendly method to attain a high-quality  $\text{SiO}_x$  layer at low temperature ( $<100^\circ\text{C}$ ) and pressure ( $<4 \times 10^4$  Pa) is by using ozone oxidation [27]. Plasma-assisted  $\text{N}_2\text{O}$  oxidation (PANO) integrated with tube plasma-enhanced chemical vapor deposition (PECVD) [26] is low cost, usually for the industrial production TOPCon [28]. Nitric acid and sulfur acid solution oxidized (NAOS)  $\text{SiO}_x$  to develop stable oxide film at 60 °C [29], as well as ultraviolet photo-oxidation (UV/ $\text{O}_3$ ) [30] depending on additional UV source can grow  $\text{SiO}_x$  layer even polysilicon at ambient temperature. The minimum recombination velocity (10 m/s) at the surface can be obtained to develop  $\text{SiO}_x$  films by thermal oxide (TO) [24]. These methods produce excellent passivation for polished c-Si surfaces, however, the passivation is severely degraded for textured surfaces [31]. Furthermore,  $\text{p}^+\text{-poly-Si}/\text{SiO}_x$  stacks weaken passivation compared to  $\text{n}^+\text{-poly-Si}/\text{SiO}_x$  stacks. The chemical passivation of the nano  $\text{SiO}_x$  layer and the field passivation of poly-Si significantly reduce the recombination at the wafer surface. On the other hand, the ultra-thin  $\text{SiO}_x$  layer ensures efficient tunneling of the carriers, and increases the open-circuit voltage ( $V_{oc}$ ) and fill factor (FF) of TOPCon solar cells.

The effective TOPCon passivation structure with the thickness of the  $\text{SiO}_x$  layer is about 1.3~1.5 nm. Table 2 is dedicated to the thickness of  $\text{SiO}_x$  film by different oxidation technologies.  $\text{SiO}_x$  has a positive charge and can be used to

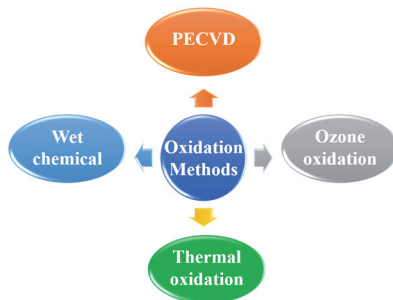


**Fig. 5.** Different techniques to fabricate the ultra-thin silicon oxide layer.

**Table 2.** The thickness of  $\text{SiO}_x$  film by different oxidation technologies [24].

| Method of oxidation | Thickness of $\text{SiO}_x$ (nm) | $T_{\text{annealing}}$ ( $^\circ\text{C}$ ) | $V_{oc}$ (mV) | $J_0$ ( $\text{fA}/\text{cm}^2$ ) | Eff (%) |
|---------------------|----------------------------------|---|---------------|-----------------------------------|---------|
| Wet chemical        | 1.2                              | 950   | 714           | 20                                | 14.5    |
|                     | 1.3~1.5                          | 800~900                                     | 719           | -                                 | 24.9    |
| Thermal oxidation   | 1.7                              | 800~1,000                                   | 705           | 50                                | 25.3    |
|                     | 1.5                              | 850   | 705           | -                                 | 21.4    |
| PECVD               | 1.55                             | 850   | 697           | -                                 | 23.0    |
|                     | 2.5                              | 800   | -             | 3.4                               | -       |
|                     | 1.1~1.4                          | 880   | -             | -                                 | -       |
|                     | 2                                | 850~880                                     | 719           | 4.3                               | 22.8    |
|                     | 1.2~1.4                          | 900   | -             | 15                                | -       |
| $\text{DIO}_3$      | 1.3~1.4                          | 900   | 715           | 35                                | -       |

passivate the n-type emitter, and the interface state density of the SiO<sub>x</sub> film is the lowest, its fixed charge is also lower than that of other oxide films (SiN<sub>x</sub> and AlO<sub>x</sub>), and will not form inversion layer when it is in contact with p-type silicon. Therefore, SiO<sub>x</sub> can be used as passivation material for p-type wafers.

#### 4. POLYSILICON LAYER AND RECENT IMPROVEMENT

##### 4.1 Role of the polysilicon layer

Compared with the back surface field (BSF) and passivated emitter rear contact (PERC) [32] based on the conventional metal-semiconductor contact and homojunction, the new generation solar cells need to handle the recombination losses and contact resistivity ( $\rho_c$ ), which mainly affect the efficiency and economic cost. Polysilicon (poly-Si) is the fundamental surface passivation material used to achieve carrier selective collection and enhance the passivating contact. Figure 6 reveals the energy band structure of the carrier selective collection used for poly-Si layers. On the surface of the

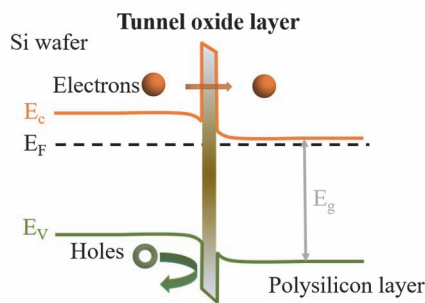


Fig. 6. Band diagram of TOPCon passivated contact technologies.

TOPCon structure, the poly-Si layer not only reduces the dangling bond density at the surface of the wafer but also affects the metal layer and is compatible with other cells, such as IBC and HIT, etc. Consequently, it is the key point to design a suitable poly-Si layer.

The poly-silicon layer (poly-Si) plays a crucial role in field passivation [33], parasitic absorption [10], impurities gathering [34], and the contact resistivity ( $\rho_c$ ) between the passivation layer and metal paste [1], which are necessary for tunneling passivation. The polysilicon layer can significantly improve the conductivity of majority carriers and the doped poly-Si enables separation of Fermi levels in the silicon wafer (high  $V_{oc}$ ) [1], which can block the transfer of minority carriers effectively, enhance majority charge carriers transport capability (high FF) and achieve selective collection of carriers [35-38].

Compared with traditional solar cells, the TOPCon structure, which relies on the SiO<sub>x</sub>/poly-silicon layer between the wafers and metallic terminal, satisfies the dangling bond density and reduces the surface recombination loss. In industrial mass production, the poly-Si layer is grown by low-pressure chemical vapor deposition (LPCVD), a sputtering method, and PECVD, the comparison of advantages and disadvantages are listed in Table 3. The *ex-situ* developed poly-Si layer by LPCVD exhibited excellent performance of passivated with the low value of saturation current density ( $J_{0,s}$ ) is 2.3 fA/cm<sup>2</sup> and minimum screen printing metalized regions is 65.8 fA/cm<sup>2</sup>. It is found that the efficiency of a large-area (244.3 cm<sup>2</sup>) p-PERC TOPCon solar cell with phosphorus-doped polysilicon (poly-Si) contact layer fabricated by LPCVD can reach 24.3% [39]. The value of  $J_{0,s}$  is 60 fA/cm<sup>2</sup> and the implied open-circuit voltage ( $iV_{oc}$ ) is 700 mV as well as the efficiency can be increased to 21.2% with the corresponding passivated p-TOPCon grown 240 nm-thick poly-Si films [40].

Table 3. Comparison of advantages and disadvantages of poly-Si layer preparation methods.

| Methods    | Advantages  | Disadvantages  |
|------------|---|--|
| LPCVD      | High output, can directly prepare an n-type polysilicon layer | It will produce winding plating, and the efficiency is relatively low        |
| PECVD      | Can be prepared on one side with high efficiency              | Low output, high requirements on equipment, and pollution to the environment |
| Sputtering | No pollution, easy and safe to operate                        | Relatively poor uniformity, high annealing temperature                       |

### 4.2 Recent improvements in the poly-silicon layer

The poly-Si on the surface of the TOPCon structure is not only significantly important for contact passivation, but also has exactly a crucial application for the tandem application of the TOPCon structure and other cells. Consequently, it is urgent to develop a new methodology used for improving the highly doped passivation. Passivating contact consists of silicon oxide (SiO<sub>x</sub>) or hydrogenated amorphous silicon (a-Si:H) located on the surface between the c-Si wafer and the metalized terminals [3], reduces the recombination and promotes the carrier's selective collection.

Conventional poly-Si/SiO<sub>x</sub> passivation depends on the high-temperature treatment for the dopant diffusing and

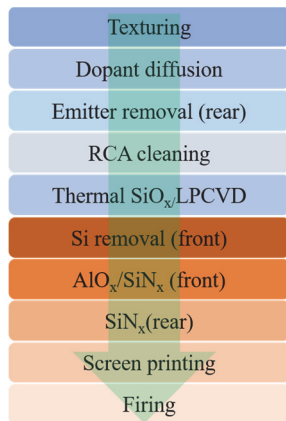


Fig. 7. Recent progress in industrial process with fired passivating contact (FPC).

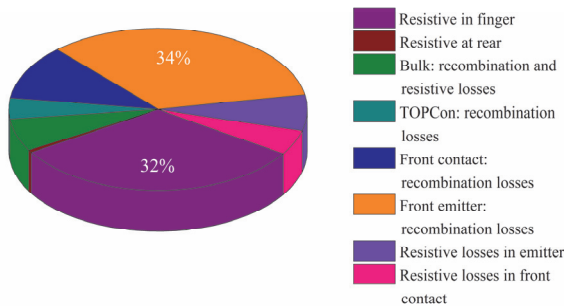


Fig. 8. The individual efficiency losses of TOPCon solar cells [47].

thermal annealing to achieve excellent passivation. Figure 7 illustrates the fired passivating contact (FPC) process, which simultaneously fabricates SiO<sub>x</sub> and introduces in-situ boron-doped PECVD a-SiC layer in the hot nitric acid atmosphere, which achieves cost-competitiveness for industrial production [41]. In the FPC process with screen printing, the recombination current density (J<sub>0</sub>) decreased to 4.9 fA/cm<sup>2</sup> and the value of contact resistivity fall to 7.2 mΩ·cm<sup>2</sup>. Doping carbon into the poly-silicon layer increases the optical band gap, improves the proton transmittance of the poly-Si layer, and endows the high temperature (<600 °C) annealing process [42]. The hydrogen atoms contained in water vapor diffuse to the interface between silicon oxide and c-Si substrate, and reduce the density of the dangling bonds [43,44], which can greatly improve the passivation effect of the poly-Si wafers. Ga-doped wafers [45] or dielectric tunnel passivation layer [46] without oxygen can be used to avoid the formation of B-O recombination defects and strengthen field effect passivation with the value of *i*V<sub>ov</sub>>730 mV and J<sub>0e</sub><5 fA/cm<sup>2</sup>, respectively, leading to better passivation for the p<sup>+</sup>-poly-Si/SiO<sub>x</sub> TOPCon structure.

The technologies of TOPCon solar cells made big progress in recent years, however, some limitations restricted the improvement of photovoltaic efficiency. Owing to the influence of solar cells itself, there are bulk limits, and optical and passivation technologies cannot eliminate the recombination and resistance loss, which prevent the increase in efficiency. Figure 8 is dedicated to the individual efficiency losses when the efficiency is 22.9% for the 10×10 cm<sup>2</sup> TOPCon solar cells, as is shown, the dominant efficiency losses are the resistive in the finger is about 32% and the recombination losses [47] at the front emitter is about 34%. From the industrial perspective, TOPCon needs double times metal of other cells during the metallization process, which hinders the progress of mass industrial production.

### 5. CONCLUSION

A wide range of methodologies and progress of TOPCon have been reported to achieve high photoelectric efficiency and reduce the recombination losses in solar cells. However, most of the TOPCon cells prepared currently have a p-TOPCon structure for rear passivation and boron-doped

technology on the front, which is not only complicated but also expensive. Nowadays, the optimization of TOPCon cells reduces the production cost and obtains better passivation simultaneously. The B-doped p-TOPCon structure and the O in the silicon oxide are easy to generate B-O recombination defects, which increase the recombination and reduce the passivation effect. Therefore, the development of the next TOPCon cells mainly includes the following points: (1) Optimize the p-TOPCon structure. If the p-TOPCon is good enough to be comparable to the passivation effect of the HIT, the shortcomings of the B-doped on the front surface of the cells can be ignored; (2) High-efficiency cells are fabricated by creating tandem structures in which TOPCon solar cells are used as bottom cells whereas solar cells fabricated with other wider bandgap materials such as III-V compound semiconductor or Perovskites are used as top cells.

#### ORCID

Junsin Yi <https://orcid.org/0000-0002-6196-0035>  
Suresh Kumar Dhungel <https://orcid.org/0000-0001-8255-9913>

#### ACKNOWLEDGEMENTS

This research was supported by grants from the New and Renewable Energy Technology Development Program of the Korea Institute of Energy Technology Evaluation and Planning (KETEP) funded by the Korean Ministry of Trade, Industry, and Energy (MOTIE) (Project No.20218520010100 and 20203040010320).

#### REFERENCES

- [1] K.W.A. Chee, B. K. Ghosh, I. Saad, Y. Hong, Q. H. Xia, P. Gao, J. Ye, and Z. J. Ding, *Nano Energy*, **95**, 106899 (2022). [DOI: <https://doi.org/10.1016/j.nanoen.2021.106899>]
- [2] Z. Liu, S. E. Sofia, H. S. Laine, M. Woodhouse, S. Wiegbold, I. M. Peters, and T. Buonassisi, *Energy Environ. Sci.*, **13**, 12 (2020). [DOI: <https://doi.org/10.1039/c9ee02452b>]
- [3] T. G. Allen, J. Bullock, X. Yang, A. Javey, and S. D. Wolf, *Nat. Energy*, **4**, 914 (2019). [DOI: <https://doi.org/10.1038/s41560-019-0463-6>]
- [4] C. Battaglia, X. Yin, M. Zheng, I. D. Sharp, T. Chen, S. McDonnell, A. Azcatl, C. Carraro, B. Ma, R. Maboudian, R. M. Wallace, and A. Javey, *Nano Lett.*, **14**, 967 (2014). [DOI: <https://doi.org/10.1021/nl404389u>]
- [5] J. Bullock, Y. Wan, Z. Xu, S. Essig, M. Hettick, H. Wang, W. Ji, M. Boccard, A. Cuevas, C. Ballif, and A. Javey, *ACS Energy Lett.*, **3**, 508 (2018). [DOI: <https://doi.org/10.1021/acsenenergylett.7b01279>]
- [6] U. Würfel, A. Cuevas, and P. Würfel, *IEEE J. Photovoltaics*, **5**, 461 (2015). [DOI: <https://doi.org/10.1109/JPHOTOV.2014.2363550>]
- [7] H. Yousuf, M. Q. Khokhar, S. Chowdhury, D. P. Pham, Y. Kim, M. Ju, Y. Cho, E. C. Cho, and J. Yi, *Curr. Photovoltaic Res.*, **9**, 75 (2021). [DOI: <https://doi.org/10.21218/CPR.2021.9.3.075>]
- [8] M. Q. Khokhar, S. Q. Hussain, S. Chowdhury, M. A. Zahid, D. P. Pham, S. Jeong, S. Kim, S. Kim, E. C. Cho, and J. Yi, *Energy Convers. Manage.*, **252**, 115033 (2022). [DOI: <https://doi.org/10.1016/j.enconman.2021.115033>]
- [9] J. Zhou, Q. Huang, Q. Zhao, W. Wang, X. Niu, Y. He, X. Su, Y. Zhao, and G. Hou, *Sol. Energy Mater. Sol. Cells*, **245**, 111865 (2022). [DOI: <https://doi.org/10.1016/j.solmat.2022.111865>]
- [10] Z. C. Holman, M. Filipič, B. Lipovšek, S. D. Wolf, F. Smole, M. Topič, and C. Ballif, *Sol. Energy Mater. Sol. Cells*, **120**, 426 (2014). [DOI: <https://doi.org/10.1016/j.solmat.2013.06.024>]
- [11] J. Schmidt, R. Peibst, and R. Brendel, *Sol. Energy Mater. Sol. Cells*, **187**, 39 (2018). [DOI: <https://doi.org/10.1016/j.solmat.2018.06.047>]
- [12] M. A. Green, E. D. Dunlop, G. Siefer, M. Yoshita, N. Kopidakis, K. Bothe, and X. Hao, *Prog. Photovoltaics: Res. Appl.*, **31**, 3 (2022). [DOI: <https://doi.org/10.1002/pip.3646>]
- [13] S. Sadkukhan, S. Acharya, T. Panda, N. C. Mandal, S. Bose, G. Das, S. Maity, P. Chaudhuri, S. Chakraborty, P. Chakraborty, and H. Saha, *IEEE J. Photovoltaics*, **13**, 236 (2023). [DOI: <https://doi.org/10.1109/jphotov.2023.3238270>]
- [14] M. A. Green, Y. Hishikawa, W. Warta, E. D. Dunlop, D. H. Levi, J. Hohl-Ebinger, and A.W.Y. Ho-Baillie, *Prog. Photovoltaics: Res. Appl.*, **26**, 668 (2017). [DOI: <https://doi.org/10.1002/pip.2909>]
- [15] F. Haase, C. Hollemann, S. Schäfer, A. Merkle, M. Rienäcker, J. Krügener, R. Brendel, and R. Peibst, *Sol. Energy Mater. Sol. Cells*, **186**, 184 (2018). [DOI: <https://doi.org/10.1016/j.solmat.2018.06.020>]
- [16] F. Feldmann, M. Bivour, C. Reichel, M. Hermle, and S. W. Glunz, *Sol. Energy Mater. Sol. Cells*, **120**, 270 (2014). [DOI: <https://doi.org/10.1016/j.solmat.2013.09.017>]
- [17] A. Richter, R. Müller, J. Benick, F. Feldmann, B. Steinhäuser, C. Reichel, A. Fell, M. Bivour, M. Hermle, and S. W. Glunz, *Nat. Energy*, **6**, 429 (2021). [DOI: <https://doi.org/10.1038/s41560-021-00805-w>]
- [18] S. Schäfer, F. Haase, C. Hollemann, J. Hensen, J. Krügener, R. Brendel, and R. Peibst, *Sol. Energy Mater. Sol. Cells*, **200**, 110021 (2019). [DOI: <https://doi.org/10.1016/j.solmat.2019.110021>]
- [19] W. Long, S. Yin, F. Peng, M. Yang, L. Fang, X. Ru, M. Qu, H. Lin, and X. Xu, *Sol. Energy Mater. Sol. Cells*, **231**, 111291

- (2021). [DOI: <https://doi.org/10.1016/j.solmat.2021.111291>]
- [20] M. Köhler, M. Pomaska, P. Procel, R. Santbergen, A. Zamchiy, B. Macco, A. Lambertz, W. Duan, P. Cao, B. Klingebiel, S. Li, A. Eberst, M. Luysberg, K. Qiu, O. Isabella, F. Finger, T. Kirchartz, U. Rau, and K. Ding, *Nat. Energy*, **6**, 529 (2021). [DOI: <https://doi.org/10.1038/s41560-021-00806-9>]
- [21] J. Zhou, Q. Huang, Y. Ding, G. Hou, and Y. Zhao, *Nano Energy*, **92**, 106712 (2022). [DOI: <https://doi.org/10.1016/j.nanoen.2021.106712>]
- [22] A. Richter, S. W. Glunz, F. Werner, J. Schmidt, and A. Cuevas, *Phys. Rev. B*, **86**, 165202 (2012). [DOI: <https://doi.org/10.1103/PhysRevB.86.165202>]
- [23] F. Feldmann, M. Bivour, C. Reichel, H. Steinkemper, M. Hermle, and S. W. Glunz, *Sol. Energy Mater. Sol. Cells*, **131**, 46 (2014). [DOI: <https://doi.org/10.1016/j.solmat.2014.06.015>]
- [24] H. Yousuf, M. Q. Khokhar, M. A. Zahid, M. Rabelo, S. Kim, D. P. Pham, Y. Kim, and J. Yi, *Energies*, **15**, 5753 (2022). [DOI: <https://doi.org/10.3390/en15155753>]
- [25] H. Tong, M. Liao, Z. Zhang, Y. Wan, D. Wang, C. Quan, L. Cai, P. Gao, W. Guo, H. Lin, C. Shou, Y. Zeng, B. Yan, and J. Ye, *Sol. Energy Mater. Sol. Cells*, **188**, 149 (2018). [DOI: <https://doi.org/10.1016/j.solmat.2018.09.001>]
- [26] D. Ma, W. Liu, M. Xiao, Z. Yang, Z. Liu, M. Liao, Q. Han, H. Cheng, H. Xing, Z. Ding, B. Yan, Y. Wang, Y. Zeng, and J. Ye, *Sol. Energy*, **242**, 1 (2022). [DOI: <https://doi.org/10.1016/j.solener.2022.07.003>]
- [27] C. K. Fink, K. Nakamura, S. Ichimura, and S. J. Jenkins, *J. Phys.: Condens. Matter*, **21**, 183001 (2009). [DOI: <https://doi.org/10.1088/0953-8984/21/18/183001>]
- [28] Y. Huang, M. Liao, Z. Wang, X. Guo, C. Jiang, Q. Yang, Z. Yuan, D. Huang, J. Yang, X. Zhang, Q. Wang, H. Jin, M. Al-Jassim, C. Shou, Y. Zeng, B. Yan, and J. Ye, *Sol. Energy Mater. Sol. Cells*, **208**, 110389 (2020). [DOI: <https://doi.org/10.1016/j.solmat.2019.110389>]
- [29] H. K. Asuha, O. Maida, M. Takahashi, and H. Iwasa, *J. Appl. Phys.*, **94**, 7328 (2003). [DOI: <https://doi.org/10.1063/1.1621720>]
- [30] A. Moldovan, F. Feldmann, G. Krugel, M. Zimmer, J. Rentsch, M. Hermle, A. Roth-Fölsch, K. Kaufmann, and C. Hagendorf, *Energy Procedia*, **55**, 834 (2014). [DOI: <https://doi.org/10.1016/j.egypro.2014.08.067>]
- [31] A. Ingenito, G. Nogay, J. Stuckelberger, P. Wyss, L. Gnocchi, C. Allebé, J. Horzel, M. Despeisse, F. J. Haug, P. Löper, and C. Ballif, *IEEE. J. Photovoltaics*, **9**, 346 (2019). [DOI: <https://doi.org/10.1109/JPHOTOV.2018.2886234>]
- [32] N. Balaji, D. Lai, V. Shanmugam, P. K. Basu, A. Khanna, S. Duttagupta, and A. G. Aberle, *Sol. Energy*, **214**, 101 (2021). [DOI: <https://doi.org/10.1016/j.solener.2020.11.025>]
- [33] Y. Zeng, D. Ma, Z. Liu, M. Liao, M. Xiao, H. Xing, N. Lin, Z. Ding, H. Cheng, Y. Wang, W. Liu, B. Yan, and J. Ye, *Mater. Sci. Semicond. Process.*, **150**, 106966 (2022). [DOI: <https://doi.org/10.1016/j.mssp.2022.106966>]
- [34] A. Y. Liu, Z. Yang, F. Feldmann, J. I. Polzin, B. Steinhauser, S. P. Phang, and D. Macdonald, *Sol. Energy Mater. Sol. Cells*, **230**, 111254 (2021). [DOI: <https://doi.org/10.1016/j.solmat.2021.111254>]
- [35] F. Feldmann, M. Simon, M. Bivour, C. Reichel, M. Hermle, and S. W. Glunz, *Sol. Energy Mater. Sol. Cells*, **131**, 100 (2014). [DOI: <https://doi.org/10.1016/j.solmat.2014.05.039>]
- [36] R. Varache, C. Leendertz, M. E. Gueunier-Farret, J. Haschke, D. Muñoz, and L. Korte, *Sol. Energy Mater. Sol. Cells*, **141**, 14 (2015). [DOI: <https://doi.org/10.1016/j.solmat.2015.05.014>]
- [37] D. Yan, A. Cuevas, J. Bullock, Y. Wan, and C. Samundsett, *Sol. Energy Mater. Sol. Cells*, **142**, 75 (2015). [DOI: <https://doi.org/10.1016/j.solmat.2015.06.001>]
- [38] Y. Zeng, H. Tong, C. Quan, L. Cai, Z. Yang, K. Chen, Z. Yuan, C. H. Wu, B. Yan, P. Gao, and J. Ye, *Sol. Energy*, **155**, 654 (2017). [DOI: <https://doi.org/10.1016/j.solener.2017.07.014>]
- [39] D. Ding, Y. Zhuang, Y. Cui, Y. Zhang, Z. Li, X. Zhang, Z. Ji, D. Wang, Y. Wan, and W. Shen, *Phys. Status Solidi RRL*, **15**, 2000455 (2020). [DOI: <https://doi.org/10.1002/pssr.202000455>]
- [40] S. Mark, D. Herrmann, M. Lenes, M. Renes, and A. Wolf, *Sol. RRL*, **5**, 2011152 (2021). [DOI: <https://doi.org/10.1002/solr.202100152>]
- [41] M. Firat, H. S. Radhakrishnan, S. Singh, F. Duerinckx, M. R. Payo, L. Tous, and J. Poortmans, *Sol. Energy Mater. Sol. Cells*, **240**, 111692 (2022). [DOI: <https://doi.org/10.1016/j.solmat.2022.111692>]
- [42] Y. Lin, Z. Yang, Z. Liu, J. Zheng, M. Feng, Y. Zhi, L. Lu, M. Liao, W. Liu, D. Ma, Q. Han, H. Cheng, Q. Zeng, Z. Yuan, B. Yan, Y. Zeng, and J. Ye, *Energy Environ. Sci.*, **14**, 6406 (2021). [DOI: <https://doi.org/10.1039/D1EE02011K>]
- [43] Z. Rui, Y. Zeng, X. Guo, Q. Yang, Z. Wang, C. Shou, W. Ding, J. Yang, X. Zhang, Q. Wang, H. Jin, M. Liao, S. Huang, B. Yan, and J. Ye, *Sol. Energy*, **194**, 18 (2019). [DOI: <https://doi.org/10.1016/j.solener.2019.10.064>]
- [44] B. Hoex, S.B.S. Heil, E. Langereis, M.C.M. van de Sanden, and W.M.M. Kessels, *Appl. Phys. Lett.*, **89**, 042112 (2006). [DOI: <https://doi.org/10.1063/1.2240736>]
- [45] D. L. Young, B. G. Lee, D. Fogel, W. Nemeth, V. LaSalvia, S. Theingi, M. Page, M. Young, C. Perkins, and P. Stradins, *IEEE. J. Photovoltaics*, **7**, 1640 (2017). [DOI: <https://doi.org/10.1109/JPHOTOV.2017.2748422>]
- [46] T. Sugiura, S. Matsumoto, and N. Nakano, *Sol. Energy*, **214**, 205 (2021). [DOI: <https://doi.org/10.1016/j.solener.2020.11.032>]
- [47] F. Feldmann, B. Steinhauser, V. Arya, A. Büchler, A. A. Brand, S. Kluska, M. Hermle, and S. W. Glunz, *33rd European Photovoltaic Solar Energy Conference and Exhibition (Fraunhofer Institute for Solar Energy Systems ISE, Amsterdam, The Netherlands, 2017)* p. 465. [DOI: <https://www.researchgate.net/publication/324537506>]